Mechanical Transients of Single Toad Stomach Smooth Muscle Cells

Effects of Lowering Temperature and Extracellular Calcium

MINEO YAMAKAWA, DAVID E. HARRIS, FREDRIC S. FAY, and DAVID M. WARSHAW

From the Department of Physiology and Biophysics, University of Vermont, College of Medicine, Burlington, Vermont 05405

ABSTRACT Smooth muscle's slow, economical contractions may relate to the kinetics of the crossbridge cycle. We characterized the crossbridge cycle in smooth muscle by studying tension recovery in response to a small, rapid length change (i.e., tension transients) in single smooth muscle cells from the toad stomach (*Bufo marinus*). To confirm that these tension transients reflect crossbridge kinetics, we examined the effect of lowering cell temperature on the tension transient time course. Once this was confirmed, cells were exposed to low extracellular calcium ($[Ca^{2+}]_o$) to determine whether modulation of the cell's shortening velocity by changes in $[Ca^{2+}]_o$ reflected the calcium sensitivity of one or more steps in the crossbridge cycle. Single smooth muscle cells were tied between an ultrasensitive force transducer and length displacement device after equilibration in temperature-controlled physiological saline having either a low (0.18 mM) or normal (1.8 mM) calcium concentration. At the peak of isometric force, after electrical stimulation, small, rapid (≤1.8% cell length in 3.6 ms) step stretches and releases were imposed. At room temperature (20°C) in normal $[Ca^{2+}]_o$, tension recovery after the length step was described by the sum of two exponentials with rates of 40–90 s^{-1} for the fast phase and 2–4 s^{-1} for the slow phase. In normal $[Ca^{2+}]_o$ but at low temperature (10°C), the fast tension recovery phase slowed (apparent $Q_{10} = 1.9$) for both stretches and releases whereas the slow tension recovery phase for a release was only moderately affected (apparent $Q_{10} = 1.4$) while unaffected for a stretch. Dynamic stiffness was determined throughout the time course of the tension transient to help correlate the tension transient phases with specific step(s) in the crossbridge cycle. The dissociation of tension and stiffness, during the fast tension recovery phase after a release, was interpreted as evidence that this recovery phase resulted from both the transition of crossbridges from a low- to high-force producing state as well as a transient detachment of crossbridges. From the temperature studies and dynamic stiffness measurements, the slow tension recovery

Address reprint requests to Dr. David M. Warshaw, Department of Physiology and Biophysics, University of Vermont, College of Medicine, Given Building, Burlington, VT 05405.

J. GEN. PHYSIOL. © The Rockefeller University Press · 0022-1295/90/04/0697/19 $2.00
Volume 95 April 1990 697–715

phase most likely reflects the overall rate of crossbridge cycling. From the tension transient studies, it appears that crossbridges cycle slower and have a longer duty cycle in smooth muscle. In low $[Ca^{2+}]_o$ at 20°C, little effect was observed on the form or time course of the tension transients. These data may indicate that the calcium dependence of the maximum shortening velocity (V_{max}) (Warshaw, D. M., S. S. Work, and W. J. McBride. 1987*b*. *Pflügers Archiv.* 410:185–191) reflects the calcium sensitivity for one or more steps in the crossbridge cycle that are rate limiting for V_{max} but are not expressed in tension transients. An alternative explanation is the existence of an internal load within the cell that impedes crossbridge cycling as the cell shortens.

INTRODUCTION

In smooth muscle, force production and shortening result from the cyclic interaction of myosin crossbridges with actin filaments (Murphy, 1980; Fay et al., 1981; Hellstrand and Paul, 1982). When compared with fast skeletal muscle, smooth muscle contracts slower and generates comparable or greater stress (i.e., force per cross-sectional area of muscle) but with far less myosin than in skeletal muscle (Cohen and Murphy, 1979). In addition, the maximum velocity of shortening in smooth muscle can be modulated by changes in extracellular calcium (Warshaw et al., 1987*b*; Siegman et al., 1984). These mechanical characteristics may reflect inherent differences in the crossbridge cycle of smooth muscle relative to skeletal muscle. For example, the slow and highly economical stress production of smooth muscle could be the result of a crossbridge that cycles slower and spends a greater percentage of its cycle in an attached force-generating state as compared with skeletal muscle (Warshaw and Fay, 1983*a*). In addition, the modulation of shortening velocity with changes in extracellular calcium concentration may reflect the calcium sensitivity of one or more steps in the crossbridge cycle. To address these possibilities, information about the kinetics of the crossbridge cycle is required. This information may be obtained by studying the time course of tension recovery after a small, rapid length change (i.e., tension transients) (Huxley and Simmons, 1971).

Recently, we recorded multiphasic tension transients in single smooth muscle cells that were qualitatively similar to those observed in skeletal muscle (Warshaw and Fay, 1983*a*,*b*; Warshaw et al., 1988). We believe that these tension transients in smooth muscle cells are dominated by processes originating within the crossbridge based on variations in cell stiffness and tension transient recovery rates that were observed during the time course of force development after stimulation (Warshaw et al., 1988). To further explore the extent to which these tension transients in single smooth muscle cells reflect active crossbridge properties, we performed experiments to address the following questions: (*a*) Are the rates of tension recovery after a length step sensitive to changes in temperature? (*b*) Do the tension recovery phases relate to specific steps in the crossbridge cycle? and (*c*) Are one or more steps in the crossbridge cycle calcium sensitive?

METHODS

Single-Cell Preparation and Instrumentation

Intact single smooth muscle cells were enzymatically isolated from the toad (*Bufo marinus*) stomach muscularis and prepared for mechanical studies as previously described (Fay et al.,

1982; Warshaw and Fay, 1983*a*). In brief, a single cell was attached between an ultrasensitive force transducer and a piezoelectric length driver. The attachment procedure, which required knotting the cell to the recording system under the microscope, was performed at room temperature in amphibian physiological saline (APS; Warshaw and Fay, 1983*a*) having either normal (1.8 mM) or low (0.18 mM) extracellular calcium. To tighten the knots at the ends of the cell, relaxed cells were stretched to a length (L_{cell}) at which a transient passive tension of ~0.2 μN was observed (Warshaw et al., 1987*b*). To activate the cell, transverse electric field stimulation was applied through platinum paddles (cross-sectional area, 0.2 mm^2). A 1-Hz electrical pulse (60 V, 0.1 ms duration) produced and maintained maximal isometric force for >30 s.

The force transducer, built in this laboratory, had the following characteristics: sensitivity, 40 mV/μN; compliance, 0.04 μm/μN; resonant frequency, 370.0 Hz; effective mass of the moving parts, 1.0 mg; damping time constant, 51 ms; noise, 2.0 mV peak-to-peak. The force transducer was calibrated at the end of every experiment and its mechanical characteristics were determined. The movement of the piezoelectric displacement device was controlled by computer. Both force and length signals were stored on FM tape and later digitized at 2,500 samples per second by a 12-bit A/D converter for subsequent computer analysis.

Length-Change Protocol

Tension responses to cell length changes were obtained by imposing a series of small, rapid step stretches and releases (0.6–1.8% L_{cell}, complete in <3.6 ms). Each length step was maintained for 1 s. These length changes were applied to the relaxed cell and then after activation at the peak of isometric force. The length-step protocol contained an ordered sequence of paired 1.8, 1.1, and 0.6% L_{cell} stretches and releases which was followed by a pseudo-random sequence of these length steps. This entire protocol lasted 16 s, during which time no detectable slowing of the tension recovery rates occurred.

In experiments in which dynamic cell stiffness was estimated during the recovery of tension after a length step, sinusoidal length perturbations (200 Hz, 0.3–0.4% L_{cell}) were superimposed on the step-length change. The 200-Hz frequency was chosen to avoid excitation of the force transducer resonance. In addition, 200 Hz was sufficiently fast to minimize the amount of tension recovery that occurs during the length change (Warshaw and Fay, 1983*a*,*b*).

Temperature Control System

To determine the temperature dependence for the rates of active force production upon stimulation and tension recovery after a length step, experiments were performed at low temperature (10°C) using a specially designed microscope slide. The slide was constructed of plexiglass and glass coverslips and sealed with water-resistant silicone cement (see Fig. 1). The plexiglass and coverslips were arranged so that a thin (0.8 mm) flow-through solution chamber was created beneath the coverslip through which cold water (3–6°C) was perfused. The solution bathing the cell was placed on top of the coverslip. Due to the thinness of the glass (0.15 mm), superb temperature conduction was obtained between the chamber and cell solution, allowing the solution temperature to be controlled to within ±0.2°C in the range of 8–12°C. The solution temperature surrounding the cell was monitored by a small thermocouple probe (copper-constantan; 0.5 mm in diameter and 1.0 mm in length; Omega, Stamford, CT) embedded in epoxy and attached to the stimulating electrodes. Placement of the stimulating electrodes provided a measurement of solution temperature within 0.3 mm of the cell. Cold water was circulated through the chamber by gravitational feed (~3 ml/min) to eliminate mechanical vibrations and electrical noise associated with the use of peristaltic pumps. Using gravitational feed, the solution temperature was lowered at a rate of 7°C per min. However, solution temperature could be lowered at 2°C per second using a peristaltic pump to achieve higher flow rates through the chamber.

Data Analysis and Processing

Before the analysis of tension transients, force records were digitally filtered to remove damped resonant oscillations of the force transducer and any high frequency noise (Warshaw and Fay, 1983*a*). All digital filtering routines were based on nonrecursive convolution filters and were carefully checked for filtering artifacts by comparing the frequency and phase components of the data before and after filtering.

Dynamic stiffness measurements. Dynamic stiffness has been used to estimate the relative contribution of elastic and viscous elements to the overall stiffness of smooth muscle (Meiss, 1978). In the present study, dynamic stiffness measurements were obtained during tension recovery after a length step, to help correlate the observed tension changes with changes in the cell's viscoelastic properties. A detailed description of the stiffness analysis has been reported previously (Warshaw et al., 1988). In brief, sinusoidal length perturbations, that were imposed throughout the tension transient, and the resultant sinusoidal force responses were extracted from the original length and force records (Fig. 2; L, F) by digital band-pass

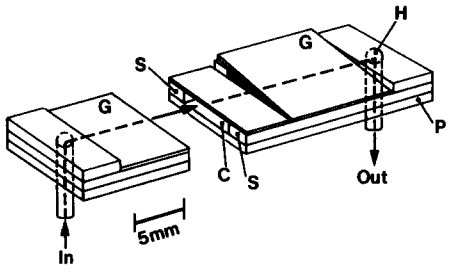

FIGURE 1. Temperature-controlling microscope slide. For illustration purposes, a transverse section and breakaway are shown. A rectangular plexiglass plate (P) serves as the base for the slide. The plate has two holes (H) at either end for inflow and outflow of the cooling fluid. Plexiglass spacers (S) span the entire length of the base plate creating a chamber (C) beneath two pieces of glass coverslip material (G). One of the coverslips is inclined relative to the horizontal plane of the slide. This incline is necessary to allow cells to be picked up by the micropipette (Warshaw and Fay, 1983*a*) without the shank of the micropipette touching the coverslip.

filtering. Using the extracted sinusoidal length and force records (Fig. 2; ΔL, ΔF), a stiffness amplitude ($\Delta F/\Delta L$, S in Fig. 7), and phase angle (ϕ in Fig. 7) between the length and force, sinusoids were calculated by Fourier series analysis on a cycle-by-cycle basis. The stiffness of a purely elastic structure exhibits a phase angle equal to zero. Therefore, any change in phase angle would indicate a change in the viscoelasticity of the cell.

As a result of the length and force sinusoid extraction, an artifact resulted in the loss of ~2.0 ms of stiffness information immediately after the completion of the length step (see S in Fig. 7). The remaining noise in the stiffness amplitude time course was due to system noise, quantization noise due to digitizing very small signal amplitudes, and the limited resolution of the Fourier expansion.

Statistical Analysis

The rates of tension and stiffness recoveries after a length step were determined by nonlinear regression analysis (P3R routine by BMDP Statistical Software, Los Angeles, CA). In previous

studies (Warshaw and Fay, 1983*b*; Warshaw et al., 1988), the majority of tension transients were fitted best by a double exponential; this was also the case in the present study. However, the recovery of stiffness after a release was best fitted by a single exponential (see Results).

To quantitate the goodness of fit, a coefficient of determination (R^2) was calculated for each fit with an acceptable fit having an R^2 value >0.8. In addition, fitted recoveries were superimposed on the original transients and visually checked to confirm the appropriateness of the fit. The tension and stiffness recovery rates from different cells were averaged by weighting each recovery rate by its inverse estimate of variance (Dixon et al., 1985). The average recovery rates are presented as a mean with an estimated standard deviation. Although the estimated standard deviation underestimates the true variance (Motulsky and Ransnas, 1987), it does serve as an excellent relative indicator of the variance.

Steady-state mechanical properties (Table I) were analyzed by ANOVA to determine if differences existed between groups. Once significance was determined by ANOVA, multiple comparisons were made between groups using Fisher's least significant difference test. Significance was accepted at $P < 0.05$.

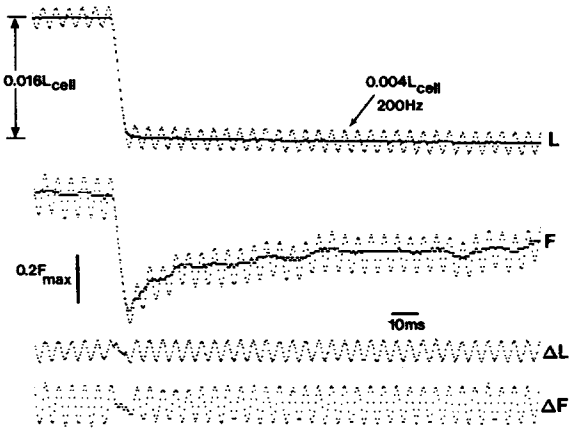

FIGURE 2. Measurement of dynamic cell stiffness during force (F) recovery in response to a release in cell length (L). Sinusoidal length changes were superimposed upon the length change. The sinusoidal length changes (ΔL) and resultant sinusoidal force changes (ΔF) were extracted by a digital bandpass filter. The dynamic cell stiffness and phase angle relationship was calculated by Fourier series analysis (see Methods). In traces L and F, the remaining cell length and force traces after sinusoidal extraction are superimposed on the original cell length and force recordings. F_{max} = 1.72 μN, L_{cell} = 88.6 μm, cell diameter = 3.4 μm.

RESULTS

Tension Transients

Single smooth muscle cells were subjected to small, rapid length changes while relaxed and then at the peak of isometric force. Typical tension responses to a 1.8% L_{cell} stretch and release in length are shown in Fig. 3 for a cell at room temperature (20°C) in normal extracellular calcium APS. Tension responses in the relaxed cell were negligible. However, in the activated cell, a significant tension increase or decrease was observed that coincided with the stretch or release, respectively. After

TABLE I

Cell parameters	Units	Extracellular solution: 20°C, 1.8 mM Ca^{2+} (n = 21)	Extracellular solution: 20°C, 0.18 mM Ca^{2+} (n = 6)	Extracellular solution: 10°C, 1.8 mM Ca^{2+} (n = 7)	ANOVA
Length (L_{cell})	μm	115 ± 8	96 ± 6	105 ± 8	—
Diameter	μm	4.6 ± 0.2	6.3 ± 0.4	3.6 ± 0.2	—
Active force (F_{max})	μN	1.4 ± 0.1	1.1 ± 0.1	1.3 ± 0.1	NS
Active stress (P_{max}) (F_{max}/cross-sectional area)	mN/mm^2	95 ± 11	39 ± 9*	125 ± 13	*
$t_{1/2}$ for force rise upon stimulation	s	3.0 ± 0.2	6.0 ± 0.4*	5.7 ± 0.7	*
Relaxed Young's modulus‡ (E_{rest})	$\times 10^4$ mN/mm^2	0.038 ± 0.004	0.009 ± 0.003*	0.063 ± 0.020	*
Active Young's modulus (E_{act})	$\times 10^4$ mN/mm^2	0.42 ± 0.05	0.14 ± 0.20*	0.47 ± 0.07	*
Shortening velocity (V_{max}§)	L_{cell}/s	0.61 ± 0.06	0.19 ± 0.01	—	

Values are ± SE. n = number of cells.

*$P < 0.05$.

‡Young's modulus (E) was calculated as follows: $E = S \times CSA/L_{cell}$, where S is cell stiffness and CSA is cell cross-sectional area.

§Warshaw et al. (1987*b*) and Warshaw (1987).

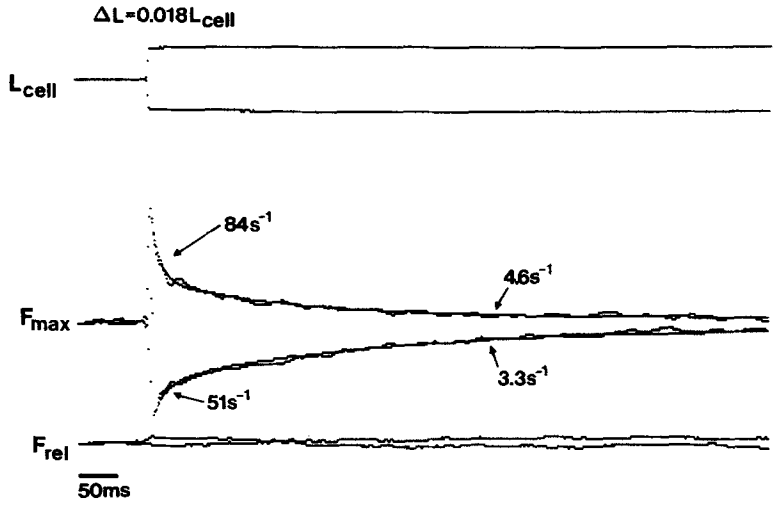

FIGURE 3. Tension transients in response to a step stretch and release in cell length (L_{cell}). The tension responses to the imposed length steps in both the relaxed (*lower trace*) and active cell (*middle trace*) are shown. In the active transients the best fit of two exponentials to the data (see Methods) are superimposed. F_{rel} = 0.0 μN, F_{max} = 1.99 μN, L_{cell} = 215.5 μm, cell diameter = 5.1 μm.

this initial elastic response, tension recovered completely within 1 s. The time course of tension recovery was best described by the sum of two exponentials with at least an order of magnitude difference in the rates for these recovery processes. The initial fast phase of tension recovery had rates of 40–90 s^{-1} with 2–4 s^{-1} for the slow tension recovery phase. The extent of tension recovery that was attributable to the fast and slow phases of recovery was approximately equal (see Fig. 6).

Tension Recovery: Dependence on Length-Step Amplitude and Direction

The recovery of tension after a length step may be related to the kinetics of the crossbridge cycle or to the viscoelasticity of structures in series with the crossbridge. In either case, the rate of tension recovery should be sensitive to the amplitude and direction of the length step. Therefore cells were subjected to a series of stretches

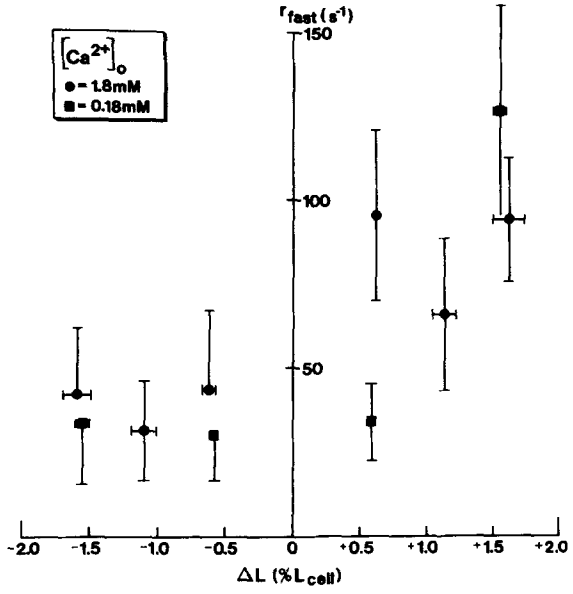

FIGURE 4. The dependence of the rate constant for the fast tension recovery phase on the amplitude and direction of the length change in both normal and low extracellular calcium. Each mean rate constant is the result of between 7 and 28 transients obtained in 6 to 16 cells.

and releases having amplitudes ranging between 0.6 and 1.8% L_{cell}, with the results presented in Figs. 4–6.

The fast phase of tension recovery exhibited a marked dependence on the amplitude and direction of the length step. The recovery rates were approximately two times faster for stretches than for releases (Fig. 4). In contrast, the rate of the slow phase of tension recovery was independent of the amplitude and direction of the length step (Fig. 5).

Temperature Effects on Force Development and Tension Transients

The contractile properties of smooth muscle cells at low temperature (10°C) in normal extracellular calcium APS are presented in Table I. The most noticeable effect on contraction due to lowering the temperature was a twofold reduction in the rate of force development after stimulation. Although cells at low temperature gener-

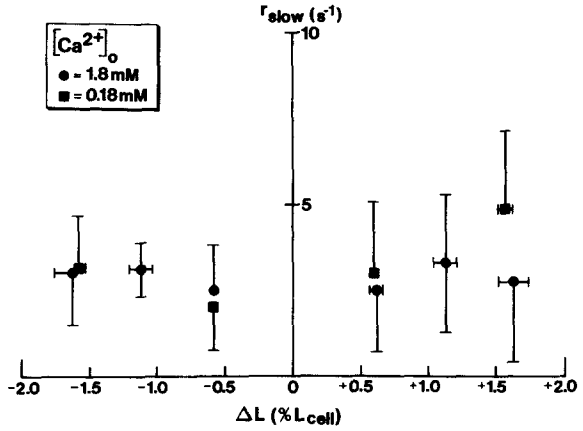

FIGURE 5. The dependence of the rate constant for the slow tension recovery phase on the amplitude and direction of the length change in both normal and low extracellular calcium. Number of transients and cells as in Fig. 4.

ated force more slowly, the maximum active stress and Young's modulus were unchanged relative to their values at room temperature (Table I). The temperature effect on force development after stimulation and the lack of any effect on active stress and Young's modulus suggest that lowering temperature may slow crossbridge cycling without affecting the number of crossbridges recruited after stimulation. However, myosin light chain phosphorylation may be rate limiting for force development after activation and thus a slower rate of crossbridge recruitment may account for the slower development of force (Kamm and Stull, 1986; Somlyo et al., 1988).

At peak isometric force, the tension recovery after a length step at low temperature was described by two exponential processes as it was at room temperature. In general, the rates of tension recovery were slower at 10°C, though there appeared to be a differential effect on the fast and slow tension recovery phases (Table II). In response to a 1.6% L_{cell} stretch and release, the rate of fast tension recovery was reduced approximately twofold. However, the slow rate of tension recovery for releases decreased a small amount with the lowering of temperature, whereas, the slow tension recovery phase for stretches was unaffected.

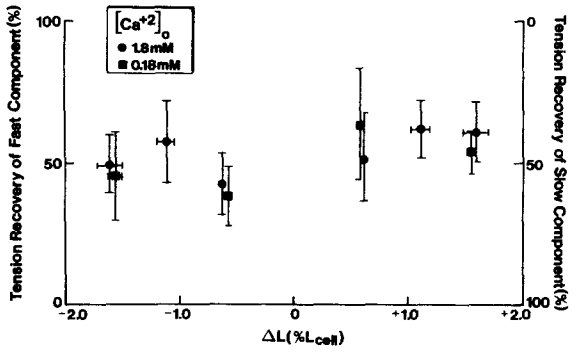

FIGURE 6. The dependence of the extent of tension recovery attributable to the fast and slow phases of recovery on the amplitude and direction of the length change in both normal and low extracellular calcium. Number of transients and cells as in Fig. 4.

TABLE II

Rates of Tension Recovery (s^{-1})

	20°C	10°C	Apparent Q_{10}
1.6% L_{cell} stretches			
r_{fast}	94.4 ± 18.6 (16)	50.2 ± 20.4 (7)	1.9
r_{slow}	2.7 ± 2.3 (16)	2.7 ± 1.7 (7)	1.0
1.6% L_{cell} releases			
r_{fast}	41.9 ± 19.8 (15)	22.6 ± 18.0 (6)	1.9
r_{slow}	3.0 ± 1.5 (15)	2.1 ± 1.5 (6)	1.4

Values are ± SD. The number in parentheses is the number of cells. Apparent Q_{10} was calculated by dividing the rate constant's mean value at 20°C by its mean value at 10°C.

Dynamic Stiffness Changes during Tension Recovery

To estimate the change in the relative number of attached crossbridges during the recovery of tension after a length step, we measured dynamic stiffness throughout the tension transient. The simultaneous tension (F), stiffness amplitude (S), and phase angle (ϕ) changes in response to a 1.6% L_{cell} step stretch and release are shown in Fig. 7. The tension transients have been digitally processed to remove the small force oscillations that occurred in response to the 200-Hz sinusoidal length perturbation (see Methods, Fig. 2). In response to a 1.6% L_{cell} stretch, tension increased by 0.58 ± 0.09 F_{max} (n = 3) and then recovered to the tension level that existed before the length step. At the same time, cell stiffness increased by 0.12 ± 0.08 S_{max} (n = 3) within 50 ms but remained elevated throughout the entire time that the stretch was maintained. No detectable change in the phase angle ($\phi = -5.3 \pm 4.0°$, n = 5) was observed during the tension transient. In response to a 1.6% L_{cell} release, tension fell

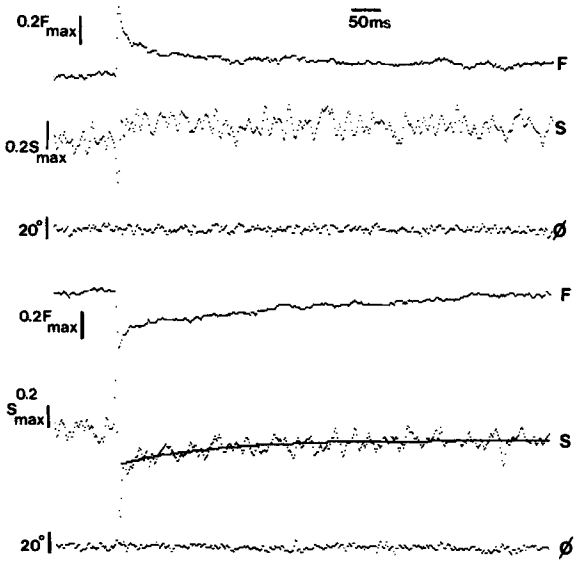

FIGURE 7. Force (F), dynamic cell stiffness, (S), and phase shift (ϕ) for a 1.6% stretch and release in cell length. The upper three traces are associated with the response to a stretch, whereas, the lower three traces are the responses to a release. The average phase angle for both stretch and release is −11°. F_{max} = 1.72 μN, L_{cell} = 88.6 μm, cell diameter = 3.4 μm.

by 0.54 ± 0.09 F_{max} (n = 4) and then recovered as described above by the sum of two exponentials (fast phase, 28.5 ± 25.3 s^{-1}; slow phase, 2.2 ± 0.7 s^{-1}; n = 4). Cell stiffness fell by 0.30 ± 0.16 S_{max} (n = 4) as a result of the release, but in contrast to the time course of tension recovery, stiffness recovery to its prerelease level was best described by a single exponential with a rate of 2.3 ± 0.5 s^{-1} (see Figs. 7 and 8 *A*). Once again, the phase angle was unchanged during the tension transient in response to the release.

Extracellular Calcium: Effects on Force Development and Tension Transients

The gross structural and mechanical characteristics of smooth muscle cells exposed to 0.18 mM calcium APS at room temperature are presented in Table I and compared with cells studied in 1.8 mM calcium APS. Although the larger cell diameters in low extracellular calcium could be interpreted as swelling due to the change in extracellular calcium, we do not believe this is the case. In a previous study (Warshaw et al., 1987*b*), no difference in cell diameter was observed for cells in normal and low extracellular calcium.

In low extracellular calcium, the relaxed Young's modulus was significantly reduced (Table I). These data may indicate that in relaxed cells, a small fraction of crossbridges are attached and their attachment is calcium dependent as was observed by Siegman et al. (1976) in rabbit taenia coli.

The rate of force development after stimulation was half the rate in normal extracellular calcium. In addition, at the peak of isometric force, both the maximum active stress and Young's modulus were ~35% of that in normal calcium, confirming our previous observations (Warshaw et al., 1987*b*).

If the reduced maximum shortening velocity in low extracellular calcium (Warshaw et al., 1987*b*) is indicative of a slower crossbridge cycling rate, then one might expect corresponding reductions in the rate of tension recovery after a length step applied to cells exposed to low extracellular calcium. These tension recoveries in response to step-length changes were once again best described by the sum of two exponentials having rate constants of 40–130 s^{-1} for the fast recovery phase and 1–5 s^{-1} for the slow phase. In addition, the tension recovery rates and percent recovery attributed to each recovery phase showed a dependence on the amplitude and direction of the length step similar to that described for cells in normal extracellular calcium at 20°C (Figs. 5–7). Therefore, no apparent effect due to lowering extracellular calcium was observed on either the form or the kinetics of tension recovery compared with that in normal extracellular calcium.

DISCUSSION

Tension Transients in Single Smooth Muscle Cells

In 1971, Huxley and Simmons reported a series of elegant experiments in which single skeletal muscle fibers were subjected to small, rapid length changes. The tension transient in response to the length step was described by an initial tension change that coincided with the length step. This elastic response was believed to originate in the crossbridge. Upon completion of the length step, tension recovered fully with a multiphasic time course that was modeled as the response of a synchro-

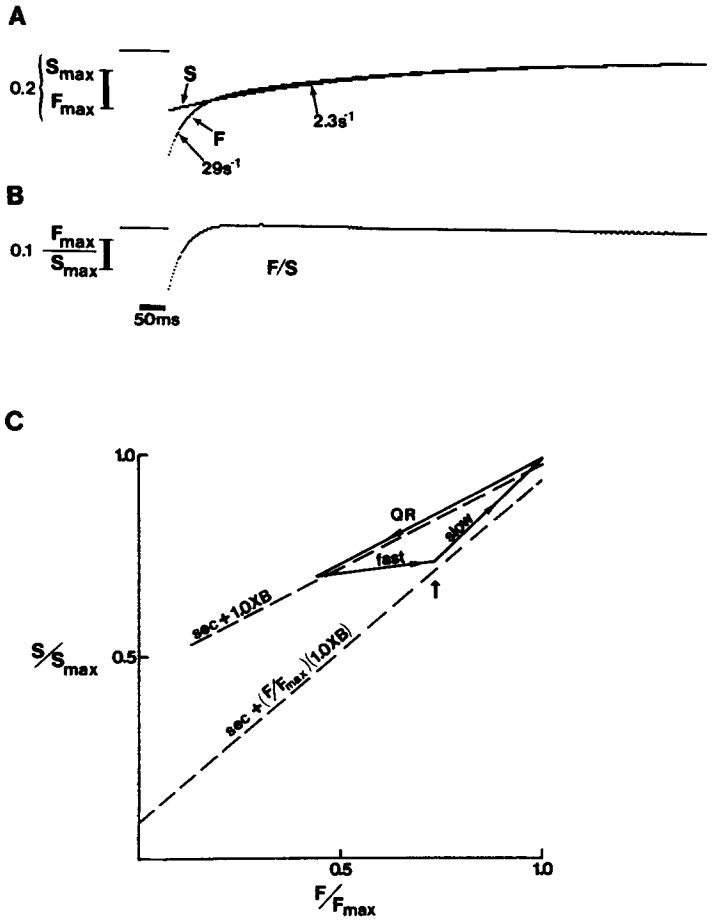

FIGURE 8. (*A*) Fitted average data for the dynamic stiffness (S) and force (F) response to a 1.6% release in length. The tension transient was fitted by two exponentials with the fast rate constant of 29 and 2.2 s^{-1} for the slow component; each process contributed equally to the tension recovery. Stiffness was fitted by a single exponential with a rate of 2.3 s^{-1}. The data were obtained from four cells. (*B*) From the data in *A*, a force-to-stiffness ratio (F/S) was calculated. (*C*) The relationship between cell stiffness (S/S_{max}) and force (F/F_{max}). Cell stiffness reflects the contribution of crossbridges (*XB*) and a series elastic component (*SEC*). The relationship between cell stiffness and force during force development after activation [*SEC* + (F/F_{max}) (1.0 *XB*)] and the relationship [*SEC* + (1.0 *XB*)] immediately after a quick release at the peak of isometric force are taken from previous studies (Warshaw and Fay, 1983*a*; Warshaw et al., 1988). The labels for these two relationships indicate the relative contributions of the crossbridges and series elastic component to cell stiffness with 1.0 *XB* representing the number of crossbridges that are attached at the peak of isometric force. Thus during force development after activation it is assumed that the number of crossbridges increases in proportion to F/F_{max}. The relationship between cell stiffness and force during the tension transient is indicated by the solid set of lines with *QR* representing the relationship during the quick release, *FAST*, the fast phase of tension recovery, and *SLOW*, the slow tension recovery phase. Since the two extreme relationships (*dashed lines*) differ only in the contributions of crossbridges to stiffness, any points that traverse between the upper and lower relationships would imply that crossbridges are detaching. Note that by the end of the fast recovery phase, where the stiffness-to-force relationship approaches the lower dashed line (*arrow*), the attached crossbridge population would have diminished by ~25% (i.e., $F/F_{max} = 0.75$).

nized population of crossbridges passing through a sequence of steps in the crossbridge cycle (Huxley and Simmons, 1971). Although biochemical studies suggest the existence of numerous crossbridge states (Lymn and Taylor, 1971; Eisenberg et al., 1980), in mechanical terms the crossbridge cycle can be characterized by three states in which the crossbridge is either detached or attached to actin in a weakly (low-force) or strongly (high-force) bound state.

The crossbridge cycle is believed to be mechanically expressed in muscle as follows: (*a*) the cycling rate is correlated to the muscle's maximum velocity of shortening (Barany, 1967); (*b*) the proportion of the cycle time spent by the crossbridge in a high-force–producing state (i.e., its duty cycle) determines, in part, the force-generating capabilities of the muscle. Smooth muscle is characterized by its slow velocity of shortening, which can be modulated by changes in extracellular calcium, and its ability to generate comparable stress, as in skeletal muscle, but with less myosin. These properties of smooth muscle may be explained if smooth muscle crossbridges cycle slower and have a greater duty cycle than in skeletal muscle. In addition, the modulation of shortening velocity by changes in extracellular calcium may be explained if one or more steps in the crossbridge cycle are sensitive to calcium. Using tension transient analysis to probe the crossbridge cycle in single smooth muscle cells, we propose to determine if crossbridges do in fact cycle slower, have a greater duty cycle than in skeletal muscle, and if rates of transition between crossbridge states are calcium sensitive.

Our previous studies have characterized tension transients in single smooth muscle cells from the toad stomach muscularis (Warshaw and Fay, 1983*a*,*b*; Warshaw et al., 1988). These initial studies suggested that the cell's elastic response to a sudden length change and the subsequent tension recovery originated predominantly within structures associated with force production. The results of the present study add additional support to this interpretation and begin to correlate both the fast and slow phases of tension recovery with specific steps in the crossbridge cycle.

Fast Tension Recovery Phase

In single smooth muscle cells at 20°C, the initial rapid phase of tension recovery can recover ~50% of the tension change resulting from the imposed length step. The temperature sensitivity of this tension recovery (apparent Q_{10} of 1.9) is interpreted as evidence that this initial rapid phase of tension recovery reflects the transition between one or more enzymatic steps in the crossbridge cycle.

In an attempt to relate the rapid tension recovery phase in smooth muscle cells to specific step(s) in the crossbridge cycle, we correlated changes in cell dynamic stiffness with tension changes during the tension transient. The time courses for tension and stiffness recovery, in response to a 1.6% release in cell length, were quite different. In contrast to the biphasic tension recovery, stiffness recovered monotonically with a rate similar to the slow phase of tension recovery (Fig. 8, *A* and *B*). The observed stiffness changes were attributed entirely to changes in cell elasticity and not to changes in cell viscosity because the stiffness phase angle was unchanged during the tension transient.

The elastic modulus in single smooth muscle cells has contributions from both attached crossbridges and an elastic element, in series with the crossbridges (War-

shaw et al., 1988). Therefore, any change in cell stiffness during the tension transient could reflect possible changes in the relative number of attached crossbridges and/or the series elastic stiffness, which is directly dependent on cell force due to its exponential length:force relationship (Warshaw and Fay, 1983*a*). To determine the contributions of crossbridge and series elasticities to the observed stiffness changes, we will rely on our previous analytical treatment of the relationship between cell stiffness and force (Warshaw et al., 1988). This treatment was based on the observation that the relationship between cell stiffness and force was not constant but rather depended on the active state of the cell. Specifically, during the development of force after activation, the relationship between cell stiffness and force differed from that at peak isometric force immediately after a quick release in cell length (Fig. 8 *C*). After activation (*lower dashed line*), cell stiffness and force are directly related and their relationship is governed by the elastic properties of the series elastic element in combination with an increasing number of attached crossbridges as they are recruited during the development of force after activation. Immediately after a quick release at the peak of isometric force (*upper dashed line*) only the elastic properties of the series elastic element determine the relationship between cell stiffness and force. This follows from the assumption that crossbridge detachment does not occur during the release, thus keeping the crossbridge contribution to cell stiffness constant. Using these two relationships, we were able to estimate changes in the attached crossbridge population by analyzing the relationship between cell stiffness and force during tension recovery.

The relationship between cell stiffness and force immediately after the release and during the recovery of force is plotted in Fig. 8 *C*. Notice that the fall in cell stiffness as a result of the release agrees with previous data from this laboratory (*upper dashed line*) (Warshaw et al., 1988). As noted previously (Warshaw et al., 1988), we believe that the fall in cell stiffness that coincides with the length step originates predominantly within the series elastic element. However, during the rapid phase of tension recovery, cell stiffness and force are no longer determined solely by the elastic properties of the series elastic element. If the series elasticity dominates the elastic response of the cell, then tension and stiffness recoveries would have identical time courses leading to a constant force-to-stiffness ratio, which is not the case (see Fig. 8, *A* and *B*). During the fast tension recovery phase, cell stiffness and force are described by a trajectory between the two extreme stiffness/force relationships (Fig. 8 *C*). These data suggest that during the fast phase of tension recovery, ~25% of attached crossbridges detach (see Fig. 8 *C*, legend). The rate of this detachment must be similar to the rate of tension recovery to counterbalance the expected increase in cell stiffness that must be occuring within the series elasticity as tension increases.

It is intriguing that cell force increases even though crossbridges may be detaching. We believe that as crossbridges detach, a significant number of crossbridges undergo a transition from a low- to high-force–producing state. A similar interpretation was proposed for the dissociation between tension and stiffness after a release in single skeletal muscle fibers (Julian and Morgan, 1981; Cecchi et al., 1982). Our interpretation is further strengthened by the similarity of the apparent Q_{10} observed for the fast phase of tension recovery in the single smooth muscle cells and that (Q_{10}

of 1.85) in single skeletal muscle fibers for the rapid tension recovery (phase 2) after a release in fiber length (Ford et al., 1977). Therefore we believe that the fast tension recovery in smooth muscle reflects both the transition between low- and high-force–producing crossbridge states as well as the simultaneous detachment of crossbridges. If these two processes occur during the fast tension recovery phase, then their combination into a single tension recovery phase may explain why these smooth muscle cells do not exhibit a tension reversal phase (i.e., phase 3) that is characteristic of tension transients from single fast skeletal muscle fibers (Ford et al., 1977). The tension reversal in skeletal muscle fibers is believed to result from the detachment of a significant number of attached crossbridges.

If the crossbridge detachment rate is similar to the rate of fast tension recovery (as predicted above), then the detachment rate may range from 40 to 90 s^{-1}. This agrees with the estimates of rigor crossbridge detachment rates (10–140 s^{-1}) obtained by flash photolysis of caged ATP in skinned portal vein (Somlyo et al., 1988). In addition, if the fast tension recovery phase in smooth muscle cells is also associated with the transition of crossbridges between low- and high-force states, then the rate of this process in smooth muscle is at least an order of magnitude slower than in fast skeletal muscle when extrapolated to the same temperature (Ford et al., 1977).

Slow Tension Recovery Phase

The slow phase of tension recovery in single smooth muscle cells accounts for the remaining 50% of the tension change that results from the imposed length step. Although it would appear that this phase of tension recovery after a release is only slightly temperature sensitive, additional experiments may be necessary to more accurately define this sensitivity. Regardless of the temperature sensitivity, the relationship between cell stiffness and force during this phase of tension recovery is no different from the relationship of cell stiffness and force that exists during force development after activation (see Fig. 8 *C*). These data would suggest that force redevelopment during the slow phase of tension recovery and force development after activation share a common mechanism which is assumed to be the attachment and cycling of crossbridges.

It is reasonable to assume that the slow rather than the fast tension recovery phase involves crossbridge cycling since the rate of the fast recovery phase is an order of magnitude greater than biochemical estimates of the crossbridge cycling rate at 25°C (Marston and Taylor, 1980; Sellers, 1985). Therefore the rate of the slow tension recovery phase sets the range for the overall cycling rate at 2–4 s^{-1} at 20°C in these single smooth muscle cells. This estimate agrees with the 1.9-s^{-1} cycling rate for actin-activated phosphorylated gizzard myosin ATPase at 25°C (Sellers, 1985) and the 4-s^{-1} cycling rate predicted from the rate of tension development after flash photolysis of caged-ATP in skinned thiophosphorylated portal vein (Somlyo et al., 1988). This estimate of crossbridge cycling is significantly lower than biochemical estimates of the cycling rate in fast skeletal muscle (Marston and Taylor, 1980) and confirms that the slower shortening velocity in smooth muscle as compared with skeletal muscle reflects an inherently slow rate of crossbridge cycling.

Dependence of the Fast Phase of Tension Recovery on the Amplitude and Direction of Length Change

Preliminary data from our laboratory suggested that the rate constant for the fast phase of tension recovery was dependent on the magnitude and direction of the length step (Warshaw and Fay, 1983*b*). This observation was confirmed in the present study with the recovery being faster for stretches than for releases. A possible explanation for the faster recovery rate after a stretch might be the existence of a viscoelastic element in series with the crossbridges. The rate constant for tension recovery in a viscoelastic system is dependent upon both the stiffness of the elastic element and the coefficient of viscosity of the viscous element. If the elastic element possessed an exponential length/force relationship, then stretching the elastic element would increase its stiffness and would therefore increase the rate constant for tension recovery. Although a viscoelasticity may exist (see above), we do not believe that its mechanical properties dominate the fast phase of tension recovery given the apparent Q_{10} of 1.9 observed for 1.6% L_{cell} stretches (see Table II).

Although we investigated dynamic stiffness changes during the tension transient in response to a stretch in an effort to relate the more rapid tension recoveries to events in the crossbridge cycle, we believe that interpretation of the slight increase in cell stiffness that was observed after a 1.6% L_{cell} stretch would be speculative at best. However, the length change dependence of the fast recovery phase in smooth muscle cells does differ from that observed in fast skeletal muscle (Ford et al., 1977), but it is similar to that in slow tortoise skeletal muscle (Heinl et al., 1974) and in cardiac muscle (Steiger, 1977). Although we can not offer an explanation why smooth, cardiac, and slow skeletal muscles share this common feature, it may underscore a common feature of the crossbridge mechanism in these muscles which relates to their slower, more economical contractions.

Distribution of Crossbridges in the Isometric Steady State

To account for the ability of smooth muscle to generate high active stresses (Dillon and Murphy, 1982) with much less myosin than in fast skeletal muscle, it is possible that the crossbridge duty cycle is greater in smooth muscle (Warshaw and Fay, 1983*a*,*b*; Warshaw, 1987). In striated muscle, the ability for complete tension recovery during the rapid recovery phase after a release in length (<0.3%) may indicate that during isometric steady state, attached crossbridges are equally distributed between attached low- and high-force–producing states (Julian et al., 1974; Eisenberg et al., 1980). This interpretation is based on the assumption that in response to a rapid release there is no net changes in the number of attached crossbridges and that complete tension recovery during the fast recovery phase can only result if sufficient numbers of low-force–producing crossbridges exist to undergo a transition between a low- and high-force state. In single smooth muscle cells, the fast phase of tension recovery after a release never achieves complete tension recovery (see Figs. 3 and 7). These data suggest that in smooth muscle the number of low-force–producing crossbridges available for the transition to the high-force state is insufficient to provide full tension recovery. However, another possible explanation is that during the rapid tension recovery phase as crossbridges undergo the low- to high-force state transition, there is a simultaneous detachment of crossbridges (as predicted

above), which would prevent tension from fully recovering. Given our estimate that 25% of the crossbridges detach during the rapid tension recovery phase, one would expect that if equal numbers of low- and high-force–producing crossbridges did exist, the tension recovery could only reach 75% at maximum. However, only a 50% recovery in tension is observed, which supports our contention that a greater percentage of attached crossbridges in single smooth muscle cells exist in the high-force–producing state (i.e., increased duty cycle) during isometric contraction. This interpretation is supported by predictions from a thermodynamic crossbridge model we have developed based on the model of Eisenberg, Hill, and Chen (1980) using single smooth muscle cell tension transient and steady-state mechanical data to constrain the model's parameters (Warshaw et al., 1984). Although an increased duty cycle may, in part, account for the stress-generating abilities of smooth muscle, we cannot rule out the possibility of a mechanical advantage imparted by the arrangement of contractile units so that more crossbridges are effectively placed in parallel within the smooth muscle cell (Ruegg, 1971; Murphy, 1980; Warshaw et al., 1987*a*; Cooke et al., 1987).

Tension Transients in Low Extracellular Calcium

The reduction in the maximum shortening velocity of cells exposed to low extracellular calcium APS (Warshaw et al., 1987*b*) suggests that the crossbridge cycling rate is reduced and may be detectable through tension transient analysis. However, to our surprise, lowering extracellular calcium did not have any effect on the form and rates of tension recovery after a length step. Although it would appear that the reduced maximum shortening velocity (V_{max}) in low extracellular calcium is not due to a direct effect of calcium on the kinetics of crossbridge cycling, it is possible that the imposed length changes do not probe steps in the crossbridge cycle that are both calcium sensitive and rate limiting for V_{max}. For instance, Guth and Junge (1982) removed calcium from contracting skinned taenia coli and observed a slower and less complete tension recovery after a small length step. They interpreted these data as evidence for a direct effect of calcium removal on the rate of crossbridge detachment. However, comparison of our results to those of Guth and Junge's (1982) may not be possible since their experiments characterized crossbridge kinetics during relaxation, which may involve different regulatory processes compared with the kinetics of crossbridge cycling during active contraction in low extracellular calcium. In skeletal muscle it is still controversial whether or not changes in intracellular calcium have any effect on crossbridge cycling (for review see Podolin and Ford, 1983).

Cells exposed to low extracellular calcium generate approximately one third the active stress and possess a Young's modulus that also is one third that in normal extracellular calcium (see Table I). These data suggest that the numbers of actively cycling crossbridges are a fraction of that in normal extracellular calcium. Therefore, an alternative explanation for the slower shortening velocities in low extracellular calcium may relate to the possible existence of a calcium-insensitive internal load within the smooth muscle cell. This internal load, which must be overcome during shortening, would place a greater effective load on the reduced number of crossbridges in low extracellular calcium and thus reduce the crossbridge's cycling

rate as predicted from the force/velocity relationship. This internal load could result in part from the compression of cytostructural elements within the cell as it actively shortens (Warshaw et al., 1987*a*). Additional support for the existence of an internal load in single smooth muscle cells is suggested by the observed slowing in velocity during isotonic shortening (Arner and Hellstrand, 1985; Warshaw, 1987; Warshaw et al., 1989). Although the effects of this internal load, as the cell shortens over considerable distances, would be mechanically expressed as a reduction in cell-shortening velocity, in the present study the small length perturbations are probably not sufficient to effect a mechanical load on the crossbridge population.

We would like to thank Whitney McBride and Janet Desrosiers for their superb technical assistance, Steven Work for many of the computer programs designed for data analysis, Trish Warshaw for her artistic talents, Guy Kennedy for the design and construction of the temperature-controlled slide, Gary Badger and Larry Haugh for their assistance in the statistical analysis, and Julie Lovelette for her expertise in desktop publishing.

This work was supported by grants from the American Heart Association and the National Institutes of Health to D. Warshaw (AR-34872 and HL-35864) and from the National Institutes of Health (HL-14523) and the Muscular Dystrophy Association to F. Fay. D. Warshaw is an Established Investigator of the American Heart Association.

Original version received 26 June 1989 and accepted version received 30 August 1989.

REFERENCES

Arner, A., and P. Hellstrand. 1985. Effects of calcium and substrate on force-velocity relation and energy turnover in skinned smooth muscle of the guinea-pig. *Journal of Physiology.* 360:347–365.

Barany, M. 1967. ATPase activity of myosin correlated with speed of muscle shortening. *Journal of General Physiology.* 50:197–218.

Cecchi, G., P. J. Griffiths, and S. Taylor. 1982. Muscular contraction: kinetics of cross-bridge attachment studied by high frequency stiffness measurements. *Science.* 217:70–72.

Cohen, D. M., and R. A. Murphy. 1979. Cellular thin filament protein contents and force generation in porcine arteries and veins. *Circulation Research.* 45:661–665.

Cooke, P. H., G. Kargacin, R. Craig, K. Fogarty, and F. S. Fay. 1987. Molecular structure and organization of filaments in single, skinned smooth muscle cells. *In* Regulation and Contraction of Smooth Muscle. M. J. Siegamn, A. P. Somlyo, and N. L. Stephens, editors. Alan R. Liss, New York, NY. 245:1–25.

Dillon, P. F., and R. A. Murphy. 1982. High force development and cross-bridge attachment in smooth muscle from swine carotid arteries. *Circulation Research.* 50:799–804.

Dixon, W. J., M. B. Brown, L. Engelman, J. W. Frane, M. A. Hill, R. I. Jennrich, and J. D. Toporek. 1985. *In* BMDP Statistical Software. University of California Press, Berkeley, CA. pp. 6 and 248.

Eisenberg, E., T. L. Hill, and Y. Chen. 1980. Cross-bridge model of muscle contraction: quantitative analysis. *Biophysical Journal.* 29:195–227.

Fay, F. S., R. Hoffman, S. Leclair, and P. Merriam. 1982. Preparation of individual smooth muscle cells from the stomach of *Bufo marinus. Methods in Enzymology.* 85:284–292.

Fay, F. S., D. D. Rees, and D. M. Warshaw. 1981. The contractile mechanism in smooth muscle. *In* Membrane Structure and Function. E. E. Bitar, editor. John Wiley & Sons, New York, NY. 4:79–130.

Ford, L. E., A. F. Huxley, and R. M. Simmons. 1977. Tension response to sudden length change in stimulated frog muscle fibres near slack length. *Journal of Physiology.* 269:441–515.

Guth, K., and J. Junge. 1982. Low Ca^{2+} impedes cross-bridge detachment in chemically skinned taenia coli. Nature. 300:775–776.

Heinl, P., H. J. Kuhn, and J. C. Ruegg. 1974. Tension responses to quick length changes of glycerinated skeletal muscle fibers from the frog and tortoise. *Journal of Physiology.* 237:243–258.

Hellstrand, P., and R. J. Paul. 1982. Vascular smooth muscle: relations between energy metabolism and mechanics. *In* Vascular Smooth Muscle: Metabolic, Ionic, and Contractile Mechanisms. M. S. Crass III and C. D. Barns, editors. Academic Press, Inc., New York, NY. 1–35.

Huxley, A. F., and R. M. Simmons. 1971. Proposed mechanism for force generation in striated muscle. *Nature.* 233:533–538.

Julian, F. J., and D. L. Morgan. 1981. Variation of muscle stiffness with tension during tension transients and constant velocity shortening in the frog. *Journal of Physiology.* 319:193–203.

Julian, F. J., K. R. Sollins, and M. R. Sollins. 1974. A model for the transient steady-state mechanical behavior of contracting muscle. *Biophysical Journal.* 14:546–562.

Kamm, K. E., and J. T. Stull. 1986. Activation of smooth muscle contraction: relation between myosin phosphorylation and stiffness. *Science.* 232:80–82.

Lymn, R. W., and E. W. Taylor. 1971. Mechanism of adenosine triphosphate hydrolysis by actomyosin. *Biochemistry.* 10:4617–4624.

Marston, S. B., and E. W. Taylor. 1980. Comparison of the myosin and actomyosin ATPase mechanisms of the four types of vertebrate muscles. *Journal of Molecular Biology.* 139:573–600.

Meiss, R. A. 1978. Dynamic stiffness of rabbit mesotubarium smooth muscle: effect of isometric length. *American Journal of Physiology.* 234:C14–C26.

Motulsky, H. J., and L. A. Ransnas. 1987. Fitting curves to data using nonlinear regression: a practical and nonmathematical review. *FASEB Journal.* 1:365–374.

Murphy, R. A. 1980. Mechanics of vascular smooth muscle. *In* Handbook of Physiology. American Physiological Society, Bethesda, MD. II:325–351.

Podolin, R. A., and L. E. Ford. 1983. The influence of calcium in shortening velocity of skinned frog muscle fibers. *Journal of Muscle Research and Cell Motility.* 4:263–282.

Ruegg, J. C. 1971. Smooth muscle tone. *Physiological Reviews.* 51:201–248.

Sellers, J. R. 1985. Mechanism of the phosphorylation-dependent regulation of smooth muscle heavy meromyosin. *Journal of Biological Chemistry.* 260:15815–15819.

Siegman, M. J., T. M. Butler, S. U. Mooers, and R. E. Davies. 1976. Calcium-dependent resistance to stretch and stress relaxation in resting smooth muscles. *American Journal of Physiology.* 231:1501–1508.

Siegman, M. J., T. M. Butler, S. U. Mooers, and A. Michalek. 1984. Ca^{2+} can affect V_{max} without changes in myosin light chain phosphorylation in smooth muscle. *Pflügers Archiv.* 401:385–390.

Somlyo, A. V., Y. Goldman, T. Fugimori, M. Bond, D. Trentham, and A. P. Somlyo. 1988. Cross-bridge kinetics, cooperatively, and negatively strained cross-bridges in vertebrate smooth muscle. *Journal of General Physiology.* 91:165–192.

Steiger, G. J. 1977. Tension transients in extracted rabbit heart muscle preparations. *Journal of Molecular and Cellular Cardiology.* 9:671–685.

Warshaw, D. M. 1987. Force:velocity relationship in single isolated toad stomach smooth muscle cells. *Journal of General Physiology.* 89:771–789.

Warshaw, D. M., R. Bisk, and F. S. Fay. 1984. A thermodynamic model of cross-bridge elasticity and kinetics from single smooth muscle cells. *Biophysical Journal.* 45:346*a*. (Abstr.)

Warshaw, D. M., and F. S. Fay. 1983*a*. Cross-bridge elasticity in single smooth muscle cells. *Journal of General Physiology.* 82:157–199.

Warshaw, D. M., and F. S. Fay. 1983*b*. Tension transients in single isolated smooth muscle cells. *Science.* 219:1438–1441.

Warshaw, D. M., W. J. McBride, and S. Work. 1987*a*. Corkscrew-like shortening in single smooth muscle cells. *Science.* 236:1457–1459.

Warshaw, D. M., S. S. Work, and W. J. McBride. 1987*b*. Effect of low extracellular calcium on shortening velocity in isolated single smooth muscle cells. *Pflügers Archiv.* 410:185–191.

Warshaw, D. M., D. D. Rees, and F. S. Fay. 1988. Characterization of cross-bridge elasticity and kinetics of cross-bridge cycling during force development in single smooth muscle cells. *Journal of General Physiology.* 91:761–779.

Warshaw, D. M., M. Yamakawa, and D. E. Harris. 1989. Evidence for an internal load in single smooth muscle cells. *In* Muscle Energetics. R. J. Paul, G. Elzinga, and K. Yamada, editors. Alan R. Liss, Inc., New York, NY. 315:329–345.